

Abstract

DANIEL EVAN PORTNER: Investigating the Seismic Gap in North Carolina: A Seismic

Survey of the Deep River Basin in Central North Carolina

(Under the direction of Dr. Lara S. Wagner)

The variability of seismic patterns in continental interiors is not well understood. A common explanation for this variability is that intraplate earthquakes concentrate on structures inherited from previous tectonic events. In the southeastern United States, seismicity concentrates in known seismic zones such as those in central Virginia, South Carolina, and eastern Tennessee. Central and eastern North Carolina, where far fewer and smaller earthquakes are recorded, lies between these regions of elevated seismicity. This pattern of seismicity is not easily explained by large-scale inherited tectonic structures. However, a lack of seismic station coverage is a potential source for the apparent quiescence of central and eastern North Carolina. In order to investigate this possibility, we deployed seismic stations across the Deep River Basin, a comparatively recent zone of extension that may be considered the most likely location for seismicity in central and eastern North Carolina. We located and calculated magnitudes for all clear seismic events between March 28, 2012 and July 3, 2013, consisting of 166 events with magnitudes ranging from M_L 0.7-1.7. The events located in four distinct clusters, with one outlier. Three of the clusters and the outlier were located near quarries and the fourth cluster was located near a large landfill site. Further, all of the events occurred on Monday-Friday between 9am and 5pm, suggesting that the events are anthropogenic. Thus, we found no evidence of natural earthquakes within our recorded magnitude range in the Deep River Basin. Additionally, using known event locations as ground-truth, we were able to test for an optimal velocity model that may be used for comparative studies of seismicity.

Acknowledgements

I would first like to thank my adviser Dr. Lara Wagner for guiding me throughout the entirety of this project. I would like to thank Dr. Diana Roman, Dr. David James, Dr. Matthew Fouch, and Steven Golden from the Department of Terrestrial Magnetism at the Carnegie Institution of Science for loaning their equipment for the PHRACCS deployment, assisting in station installation, and databasing. I would also like to thank Dorrان Howell and all of the other students at UNC-Chapel Hill who have assisted in maintaining the PHRACCS deployment. This project was supported by the Daniel Pignatiello Fellowship, administered by the Department of Geological Sciences at UNC-Chapel Hill. This project was additionally supported by a Summer Undergraduate Research Fellowship administered by the Office of Undergraduate Research at UNC-Chapel Hill.

Table of Contents

	Page
Abstract.....	ii
Acknowledgements.....	iii
List of Tables and Figures.....	v
Section	
1. Introduction.....	1
1.1. Intraplate Seismicity.....	1
1.2. The North Carolina seismic gap.....	2
1.3. The Deep River Basin and hydraulic fracturing.....	4
2. Data and Methods.....	5
2.1. Velocity model calibration.....	6
2.2. Event magnitude determination.....	7
3. Results.....	8
4. Discussion.....	11
4.1. Tectonic implications.....	11
4.2. PHRACCS detection capabilities and implications for hydraulic fracturing.....	11
5. Conclusions.....	14
6. References.....	15
7. Tables.....	22
8. Figures.....	23

List of Tables and Figures

Table	Page
1. Results of Velocity Model Testing.....	22
Figure	
1. Map of East Coast Seismicity.....	23
2. PHRACCS Station Map.....	24
3. Histogram of Events by Day of Week.....	25
4. Histogram of Events by Time of Day.....	26
5. Velocity Models.....	27
6. Histogram of Events by Local Magnitude.....	28
7. Results Map.....	29
8. Satellite Images of Event Clusters.....	30
9. Sample Seismograms.....	31
10. Event Locations for Tested Velocity Models (Part I).....	32
11. Event Locations for Tested Velocity Models (Part II).....	33
12. Event Locations for Tested Velocity Models (Part III).....	34
13. Plot of Calculated Epicenter Error.....	35

1. Introduction

1.1. Intraplate seismicity

Although most seismicity occurs along plate boundaries, significant earthquake activity occurs in intraplate settings. Natural seismicity shows strong variability in such stable continental interiors. Many workers have attempted to explain this variability, but the cause of intraplate seismicity and its spatial distribution remains enigmatic.

Some workers propose that the variability in intraplate earthquake distribution does not express meaningful patterns, but instead is the result of insufficient sampling in time of a random distribution of earthquakes (Swafford and Stein 2007, Li *et al.* 2009). Others propose that intraplate earthquakes are the result of modern processes. Bollinger (1973) propose that intraplate earthquakes occur in regions of local uplift whereas seismically quiet regions express relative subsidence and Bräuer *et al.* (2003) and Costain (2008) suggest that pore fluid overpressure is the source of intraplate earthquakes, either from CO₂ exhaled from mantle magma reservoirs or meteoric subsurface water flow following weather patterns.

However, the most pervasive explanation of the apparent patterns of intraplate seismicity is that they concentrate on structures inherited from previous tectonic events.

Associations are identified between intraplate seismicity and inherited zones of weakness from the last major orogeny (Sykes 1978), crust weakened by past extension (Dewey 1988, Johnston and Kanter 1990, Chapman and Beale 2010, and Bartholomew and Van Arsdale 2012), terrane boundaries (Babuska *et al.* 2007), cratonic boundaries (Li *et al.* 2007), extensions of major oceanic fracture zones (Fletcher *et al.* 1978), continental fracture zones (Talwani 1988, Zoback 1992), and zones of thinner or warmer mantle lithosphere (Liu and Zoback 1997, Assumpção *et al.* 2004, and Mooney *et al.* (2012).

1.2. The North Carolina seismic gap

Large-scale tectonic structures in the southeastern United States are the result of the formation and breakup of the supercontinents Rodinia and Pangaea (Thomas 2006). Rodinia formed as a result of the Grenville Orogeny (1.35-0.98 Ga) (Hoffman 1991, Rivers 1997, Thomas 2006). This event accreted the Grenville Province, which presently extends from northern Canada to Mexico along the western side of the Appalachian Mountains (Bartholomew 1983, Rivers 1997, Thomas 2006). The breakup of Rodinia occurred with the opening of the Iapetus Ocean. Extension began ~760 Ma, but the Iapetus Ocean did not open until ~550 Ma (Rankin 1976, Williams and Hiscott 1987, Thomas 2006, Hatcher 2010). The Iapetus Ocean spread on an axis subparallel to the Grenville Front (Thomas 2006). The subsequent closing of the Iapetus Ocean during the formation of Pangaea occurred over the course of three successive orogenies: the Taconic (Ordovician-Silurian), Acadian (Devonian-Mississippian), and Alleghanian (Mississippian-Permian) (Hibbard 2000, Hibbard *et al.* 2002, Thomas 2006, Miller *et al.* 2006, Hatcher 2010). This series of orogenies resulted in the formation of the Appalachian Mountains and the accretion of the Piedmont and Carolina terranes (Hibbard 2000, Hibbard *et al.* 2002, Thomas 2006). These terranes, making up the majority of the southeastern United States, accreted along the former Laurentian margin created by Iapetan seafloor spreading (Hibbard *et al.* 2002). Subsequent Mesozoic extension resulted in the opening of the Atlantic Ocean along the East Coast Magnetic Anomaly (McBride and Nelson 1988) and a series of failed rift basins along the new coastline called the Newark Supergroup (Olsen *et al.* 1989).

Each of the accreted terranes present along the passive margin in the southeastern United States extends north-south along strike from Georgia to northern Virginia (Hibbard *et al.* 2002,

Hatcher 2010). However, seismic patterns in the southeastern United States show significant spatial variations that do not appear to be correlated to observed terrane boundaries or structures (Bollinger 1973; Figure 1). Earthquakes concentrate in known seismic zones such as the Central Virginia Seismic Zone (Bollinger 1973), location of the 2011 M_w 5.8 Mineral, VA earthquake (Wolin *et al.* 2012), the South Carolina Seismic Zone (Bollinger 1973, Tarr *et al.* 1981, Dewey 1988), location of the 1886 M_w 7.3 Charleston, SC earthquake (Tarr *et al.* 1981, Talwani 1982), and the Eastern Tennessee Seismic Zone (Bollinger 1973, Powell *et al.* 1994, Chapman *et al.* 1997). Central and eastern North Carolina, where far fewer and smaller earthquakes have been recorded, lies between these regions of elevated seismicity. Between 1973 and 2006, there were 83 earthquakes M_w 2.0 or greater in Virginia and 84 in South Carolina east of the Appalachian Mountains, but only eleven in North Carolina east of the Appalachians (earthquake.usgs.gov/earthquakes/search/). This region of reduced seismicity, the North Carolina seismic gap, has been recognized for some time (Sbar and Sykes 1973, Bollinger 1973), but without correlation with major tectonic structures, it lacks an obvious tectonic explanation.

The apparent quiescence in North Carolina coincides with a lack of available passive seismic data. There are only four seismic stations east of the Appalachians in North Carolina with data included in the Incorporated Research Institutions for Seismology (IRIS) Data Management Center (DMC) database prior to this study: the Penn State Network's NCAT station, the Appalachian Seismic Transect's LARA station, and the United States National Seismic Network's CEH and CNNC stations (www.iris.edu/dms/nodes/dmc/). Thus, it is possible that the apparent sparsity of earthquakes in central and eastern North Carolina is due to insufficient station coverage. In order to investigate the hypothesis that the apparent quiescence of central and eastern North Carolina is the result of sampling error, we deploy seismic stations

around the Deep River Basin. As discussed below, the Deep River Basin is a comparatively recent zone of extension and may therefore be considered the most likely location for seismicity in central and eastern North Carolina.

1.3. The Deep River Basin and hydraulic fracturing

The Deep River Basin is one of a series of Triassic rift basins along the east coast of the United States that make up the Newark Supergroup (Olsen *et al.* 1989). The supergroup of basins formed from preliminary extension during the breakup of Pangaea before the Atlantic Ocean began to spread (Olsen *et al.* 1989). The Deep River Basin consists of three sub-basins, the Wadesboro sub-basin, the Sanford sub-basin, and the Durham sub-basin (Olsen *et al.* 1989). A bed of shale and coal known as the Cumnock formation surfaces along the northern margin of the Sanford sub-basin (Olsen *et al.* 1991). In the past, this has been exploited by coal mining operations. More recently, however, it has been the focus of local gas companies. Recent legislation suggests that hydraulic fracturing operations may occur in the Sanford sub-basin in the near future. While hydraulic fracturing itself does not cause seismicity large enough to be recorded by the type of data analyzed here, the reinjection of wastewater into basement rocks has been linked to more significant seismicity in certain areas. Although it is unknown whether or not hydraulic fracturing or the associated reinjection of wastewater will occur in the Sanford sub-basin, a baseline of natural seismicity can be recorded before operations to be used for any comparative studies of seismicity.

2. Data and Methods

In order to study the natural seismicity of the Deep River Basin, I assisted in the deployment of the Pre-Hydrofracking Regional Assessment of Central Carolina Seismicity (PHRACCS) network. This deployment consists of twelve stations in a ~50 x 50 km array with ~5-15 km station spacing throughout the Sanford sub-basin of the Deep River Basin (Figure 2). The seismometers are STS-2 broadband sensors recording at a sampling rate of 40 Hz. All of the stations, with the exception of the northernmost (NC01), westernmost (NC02), and easternmost (NC06) stations are located within the Deep River Basin.

Seismic events were detected using the `dbdetect` and `dbgrassoc` programs from Boulder Real Time Technologies' Antelope software (www.brtt.com). To detect seismic event arrivals, we employed a Short Term Average/Long Term Average (STA/LTA) ratio method. An event was detected when the threshold STA/LTA ratio of 3 was met by at least eight stations within a 1.5 second window, signifying the arrivals were likely of the same event. This low threshold identified many false signals in addition to discrete earthquake-like seismic events. To remove false signals, I filtered the detections to leave only events with an identifiable P-wave and S-wave arrival on at least eight stations.

Event hypocenters were calculated using the Hypocenter program (Leinert *et al.* 1986) included with the SEISAN seismic analysis software package (Havskov and Ottemöller 1999). For each event-station pair, I picked all discernable P-wave and S-wave arrivals on the vertical and transverse components, respectively. S-wave picks were ranked to represent pick confidence. Picks were ranked as "1" when the picks were clear and impulsive arrivals. Picks were ranked as "2" when they were clear, but not impulsive, S-wave arrivals and the precise moment of arrival was uncertain. Locations were calculated using a 1-D velocity model derived

from Bonini and Woollard (1960) and Olsen *et al.* (1991) (See 2.1. Velocity Model Calibration). Events with latitude or longitude errors greater than 5 km and events located more than 6 km outside of the array were not included in further analysis.

In order to evaluate possible sources for recorded events, I examined satellite images of the event locations on Google Maps. I then compiled histograms of event source times by local time of day and day of the week (Figures 3 and 4). As discussed in the results and discussion sections, most of the events were located near an observable quarry and all occurred during business hours, suggesting an anthropogenic source.

2.1. Velocity model calibration

Based on the assumption that the 136 events located near quarries are recorded quarry blasts, I developed an optimized 1-D velocity model for locating seismic events in the Deep River Basin. The center of each quarry is assumed to be the “true” location for events in that cluster, providing a ground truth estimate of goodness of fit between calculated event locations and the nearest quarry. In order to test for the optimized velocity model, I selected 29 events with a location confirmed by the source that had the highest number of easily picked P-wave arrivals. I then calculated the average distance between the calculated epicenter and the known source location. In order to remove error induced by depth calculations while testing various velocity models, I fixed hypocenter depths to 0 km. I removed S-wave picks with a ranking of 2 in order to use only the most reliable data for this calibration.

I relocated the events with each of the seven velocity models shown in Figure 5. These include models which test the effects of adding a 1.5 km deep slow sedimentary basin layer (Velocity Models 2-4; as identified by Olsen *et al.* 1991)). These velocity models are within the

constraints provided by Bonini and Woollard (1960), with P-wave velocities in the basin between 3.2-4.4 km/s and in the upper crust between 4.8-5.8 km/s. Mid- and lower-crustal velocities are derived from seismic refraction studies in Tennessee and Missouri and off the mid-Atlantic coast (Catchings 1999, Holbrook *et al.* 1992). The tested models vary velocities in the basin and the upper crust within the constraints of Bonini and Woollard (1960) while leaving the mid-crust through upper mantle unchanged (Figure 5). I used the best fitting velocity model (Velocity Model 1) for the final locations presented in this study.

2.2. Event magnitude determination

I calculated local event magnitudes (M_L) for each event using the MULPLT and Hypocenter (Leinert *et al.* 1986) programs within SEISAN (Havskov and Ottemöller 1999). For each event, I converted the seismograms to match the response of a Wood-Anderson seismograph using MULPLT (Havskov and Ottemöller 1999). This automatically determines maximum displacement amplitude on the vertical component of the Wood-Anderson seismogram. Using Hypocenter (Leinert *et al.* 1986), I calculated M_L for each station-event pair with distance from the event and the maximum displacement amplitude. For each event, we consider the average M_L of all stations to be the event's M_L (Figure 6). I calculated standard error for each event to analyze error in our magnitude calculations.

3. Results

After removing poorly constrained events from the dataset, I found 166 events that were locatable within or close to the PHRACCS array between March 30, 2012 and July 3, 2013. The event epicenters fall into four distinct clusters, with one exception (Figure 7). Two clusters (Clusters 1 and 2), consisting of 97 events total, are located northeast of the array. Cluster 3, consisting of 38 events, is located southeast of the array. Cluster 4, consisting of 30 events, is located in the center of the array around station NC04. The last event is located on the southwestern edge of the array.

Clusters 1, 2, and 3 are co-located with the Luck Stone Pittsboro Plant quarry, the Wake Stone Corporation quarry, and the Martin Marietta Aggregates Lemon Springs Quarry, respectively (Figure 8). Cluster 4 is located in Cumnock near the site of the abandoned Egypt Coal Mine and is not associated with an obvious quarry. All recorded events occurred between 9am and 5pm local time on Monday through Friday. The spatial and temporal association of the events with business activities suggests that the events are the result of quarry blasts and other human activities. In order to validate this association, I contacted two of the event source quarries by phone. The Luck Stone Pittsboro Plant confirmed they had an explosion coincident with the origin time of each event recorded in Cluster 1 from January to June 2013. The Wake Stone Corporation confirmed they had an explosion coincident with the origin time of each event recorded in the cluster from April 2012 to June 2013. I was unable to reach the Martin Marietta Aggregates Lemon Springs Quarry (Cluster 3). No source for Cluster 4 was contacted because its source remains ambiguous, but two observations suggest that the events are likely anthropogenic as well: 1) the 30 events in the cluster occur during business hours without

exception (Figures 3 and 4) and 2) the seismograms for these events are indiscernible from the seismograms from the confirmed quarry blasts (Figure 9).

The results of the velocity model calibration indicate that velocity models with a sedimentary basin yield significantly less accurate locations than those without a basin included (See Velocity Models 2-4 in Table 1). Figures 10, 11, and 12 show the locations calculated for each velocity model. Velocity Model 1 locates events most accurately, placing events on average 2.019 km from their respective sources. However, Velocity Model 1 located events best when depth was left free and S-wave picks ranked 2 were included in calculations, locating events on average 1.689 km from their respective sources (See Velocity Model 1a in Table 1), so locations in this study were calculated with these conditions.

Considering the known quarries as the source locations for Clusters 1, 2, 3, and the outlying event, we relocated the events with Velocity Model 1. All of the events with a known source located at their respective sources within error (Figure 13).

The calculated error for event locations using Velocity Model 1 ranges from 0.6-4.3 km in latitude and 0.9-3.8 km in longitude. Calculated hypocenter depths range from 0.7-8.1 km with 1.6-10.4 km error. However, 139 of 166 events were located within 2 km of their respective source, showing that hypocenter error is more likely on the order of 2 km using the PHRACCS array.

The results of the magnitude determinations show recorded local magnitudes of 0.7-1.7 (Figure 6). For a given station, magnitudes were calculated as low as 0.2 and as high as 2.4. An analysis of the scatter of magnitude values for each station shows that on average, each station deviates from the mean by no more than 0.2, showing that there is no large systematic error induced by a single station. The standard error for each recorded magnitude is on average less

than 0.1. This error is likely the result of variable attenuation reducing or enhancing amplitudes at a given station and/or, error in epicenter locations effecting calculated distances (described above).

4. Discussion

4.1. Tectonic implications

The apparent lack of natural seismicity in the Deep River basin strongly suggests that the observed along-strike variability in seismic moment release in the southeastern United States is not due to variable sampling. A more recent catalog of earthquakes with TA's uniform station sampling confirms the variation in seismicity (earthquake.usgs.gov/earthquakes/search/).

Determining the cause of this variability is difficult because of the lack of seismic data recorded in the region (See Introduction). A potential source for variation between North Carolina and the surrounding states is the Cape Fear Arch, a prominent feature of raised basement extending inland from the coast (Soller 1988). However, there has not been a comprehensive correlation between the Cape Fear Arch and seismic patterns. Recent seismic studies in the eastern United States have not had clear enough resolution surrounding North Carolina to identify small-scale variations in structure such as the Cape Fear Arch (van der Lee *et al.* 2008, Bedle and van der Lee 2009, Sigloch 2011).

The aforementioned studies on the causes of intraplate seismicity suggest that the Cape Fear Arch or another as yet unknown variation in inherited lithospheric structure may be able to explain the variable seismicity in the eastern United States. However, further seismic studies across the region by Earthscope's TA or FlexArray will be necessary to look at North Carolina's subsurface with higher resolution.

4.2. PHRACCS detection capabilities and implications for hydraulic fracturing

Although no natural earthquakes were recorded by the PHRACCS array, the recorded quarry blasts provide a constraint on the event detection abilities of the network. PHRACCS was

able to consistently locate quarry blasts within 2 km of their source quarry. This allows us to constrain the accuracy of the locations we are able to calculate using the array. Further, the array was able to consistently record locatable quarry blasts at $M_L > 0.8$ (Figure 6), with only four blasts $< M_L 0.9$ confidently recorded above background noise.

It is expected that hydraulic fracturing operations will occur in the Sanford sub-basin to exploit a reported large repository of shale gas in the Cumnock formation. The constraints on our ability to detect and locate events using the PHRACCS array indicate the array's utility in the event of local hydraulic fracturing and wastewater reinjection. The process of hydraulic fracturing produces many earthquakes, but these earthquakes are rarely strong enough to be felt (Ellsworth 2013). The majority of earthquakes produced by hydraulic fracturing are of moment magnitude (M_w) < 0 (Davies *et al.* 2013, Holland 2013), which is much smaller than the events located with the PHRACCS array. Traditionally, studies of microseismicity induced by hydraulic fracturing require dense arrays of borehole seismometers that can locate extremely small earthquakes within meter scale error (House 1987, Davies *et al.* 2013, Raleigh *et al.* 1976, Rutledge *et al.* 2004). PHRACCS can only locate events accurately to within 2 km, which is not precise enough to study such induced earthquakes (Davies *et al.* 2013).

The PHRACCS array will, however, be useful in the event of local wastewater reinjection. There are several cases of large earthquakes being attributed to wastewater reinjection, but there is generally not a comprehensive baseline of seismicity for comparison to confirm that earthquakes did not previously occur naturally (Holland 2013). Such earthquakes are frequently $M_w > 3$ and in some cases reach greater than $M_w 5$, such as the 2011 $M_w 5.7$ in Oklahoma (Keranen *et al.* 2013). This study provides a detailed baseline of natural seismicity in the region that Earthscope's TA, with 70 km station spacing, cannot provide. The baseline of

natural seismicity recorded by PHRACCS consists of no confirmed natural earthquakes in the Sanford sub-basin during the fifteen months analyzed for this study. The data from this study are publicly available at the IRIS DMC for future analysis if warranted by local events.

5. Conclusions

We investigate the North Carolina seismic gap by looking for previously unrecorded earthquakes with a dense array of broadband seismometers in the Triassic Deep River Basin. Due to the extensive seismicity in surrounding regions, such as the South Carolina Seismic Zone, the Central Virginia Seismic Zone, and the Eastern Tennessee Seismic Zone, we expected to record earthquakes in North Carolina. The results of this investigation can be summarized in three main conclusions:

- 1) The North Carolina seismic gap is a robust observation and is not due to a lack of regional seismic data.
- 2) The PHRACCS array confidently recorded and located seismic events down to M_L 0.9 \pm 0.1. Events can accurately be located within 2 km of their sources.
- 3) We have found no evidence of natural earthquakes with $M_L > 0.8$, in the Sanford sub-basin of the Deep River Basin between May 28, 2012 and July 3, 2013. This may be used as a baseline for comparison in later studies of the region.

6. References

- Assumpção, M., M. Schimmel, C. Escalante, J.R. Barbosa, M. Rocha, and L.V. Barros (2004). Intraplate seismicity in SE Brazil: stress concentration in lithospheric thin spots. *Geophysical Journal International*, **159**, 390-399.
- Babuska, V., J. Plomerova, and T. Fischer (2007). Intraplate seismicity in the western Bohemian Massif (central Europe): A possible correlation with a paleoplate junction. *Journal of Geodynamics*, **159(1)**, 390-399.
- Bartholomew, M.J. (1983). Palinspastic reconstruction of the Grenville terrane in the Blue Ridge Geologic Province, southern and central Appalachians, U.S.A. *Geological Journal*, **18**, 241-253.
- Bartholomew, M.J. and R.B. Van Arsdale (2012). Structural controls on intraplate earthquakes in the eastern United States. *Recent Advances in North American Paleoseismology and Neotectonics East of the Rockies*, **493**, 165-189.
- Bedle, H. and S. van der Lee (2009). S velocity variations beneath North America. *Journal of Geophysical Research*, **114**, B07308.
- Bollinger, G.A. (1973). Seismicity and crustal uplift in the southeastern United States. *American Journal of Science*, **Cooper 273-A**, 396-408.
- Bonini, W.E. and G.P. Woollard (1960). Subsurface Geology of North Carolina-South Carolina Coastal Plain from Seismic Data. *AAPG Bulletin*, **44**, 298-315.
- Bräuer, K., H. Kämpf, G. Strauch, and S.M. Weise (2003). Isotopic evidence ($^3\text{He}/^4\text{He}$, $^{13}\text{C}_{\text{CO}_2}$) of fluid-triggered intraplate seismicity. *Journal of Geophysical Research*, **108**, 2070.
- Catchings, R.D. (1999). Regional Vp, Vs, Vp/Vs, and Poisson's Ratios across Earthquake Source Zones from Memphis, Tennessee, to St. Louis, Missouri. *Bulletin of*

- Seismological Society of America*, **89**, 1591-1605.
- Chapman, M.C., C.A. Powell, G. Vlahovic, and M.S. Sibol (1997). A Statistical Analysis of Earthquake Focal Mechanisms and Epicenter Locations in the Eastern Tennessee Seismic Zone. *Bulletin of the Seismological Society of America*, **87(6)**, 1522-1536.
- Chapman, M.C. and J.N. Beale (2010). On the Geologic Structure at the Epicenter of the 1886 Charleston, South Carolina, Earthquake. *Bulletin of the Seismological Society of America*, **100**, 1010-1030.
- Costain, J.K. (2008) Intraplate Seismicity, Hydroseismicity, and Predictions in Hindsight. *Seismological Research Letters*, **79**, 578-589.
- Davies, R., G. Foulger, A. Bindley, and P. Styles (2013). Induced seismicity and hydraulic fracturing for the recovery of hydrocarbons. *Marine and Petroleum Geology*, **45**, 171-185.
- Dewey, J.W. (1988). Midplate seismicity exterior to former rift-basins. *Seismological Research Letters*, **59(4)**, 213-218.
- Ellsworth, W.L. (2013). Injection-induced earthquakes. *Science*, **341**, 1225942.
- Fletcher, J.B., M.L. Sbar, and L.R. Sykes (1978). Seismic trends and travel-time residuals in eastern North America and their tectonic implications. *Geological Society of America Bulletin*, **89**, 1656-1676.
- Hatcher, R.D. (2010). The Appalachian orogen: a brief summary. In: Tollo, R.P., M.J. Bartholomew, J.P. Hibbard, and P.M. Karabinos (Eds.), *From Rodinia to Pangea: The Lithotectonic record of the Appalachian Region*, 1-19.
- Havskov, J. and L. Ottemöller (1999). SeisAn Earthquake Analysis Software. *Seismological Research Letters*, **70**, 532-534.
- Hibbard, J. (2000). Docking Carolina: Mid-Paleozoic accretion in the southern Appalachians.

- Geology*, **58**, 127-130.
- Hibbard, J.P., E.F. Stoddard, D.T. Secor, and A.J. Dennis (2002). The Carolina Zone: overview of Neoproterozoic to Early Paleozoic peri-Gondwanan terranes along the Eastern Flank of the southern Appalachians. *Earth-Science Reviews*, **57**, 299-339.
- Hoffman, P.F. (1991). Did the Breakout of Laurentia Turn Gondwanaland Inside Out? *Science*, **252(5011)**, 1409-1412.
- Holbrook, W.S., G.M. Purdy, J.A. Collins, R.E. Sheridan, D.L. Musser, L. Glover III, M. Talwani, J.I. Ewing, R. Hawman, and S.B. Smithson (1992). Deep Velocity Structure of Rifted Continental Crust, U.S. Mid-Atlantic Margin, from Wide Angle Reflection/Refraction Data. *Geophysical Research Letters*, **19**, 1669-1702.
- Holland, A.A. (2013). Earthquakes Triggered by Hydraulic Fracturing in South Central Oklahoma. *Bulletin of the Seismological Society of America*, **103**, 1784-1792.
- House, L. (1987). Locating Microearthquakes Induced by Hydraulic Fracturing in Crystalline Rock. *Geophysical Research Letters*, **14**, 919-921.
- Johnston, A.C. and L.R. Kanter (1990). Earthquakes in Stable Continental Crust. *Scientific American*, **March**, 68-75.
- Keranen, K.M., H.M. Savage, G.A. Abers, and E.S. Cochran (2013). Potentially induced earthquakes in Oklahoma, USA: Links between wastewater injection and the 2011 M_w 5.7 earthquakes sequence. *Geology*, **41**, 699-702.
- Leinert, B.R., E. Berg, and L.N. Frazer (1986). Hypocenter: An Earthquake Location Method Using Centered, Scaled, and Adaptively Damped Least Squares. *Bulletin of the Seismological Society of America*, **76**, 771-783.
- Li, Q., M. Liu, Q. Zhang, and E. Sandvol (2007). Stress evolution and seismicity in the

- central-eastern United States: Insights from geodynamic modeling. *Geological Society of America Special Paper*, **425**, 149-166.
- Li, Q., M. Liu, and S. Stein (2009). Spatiotemporal Complexity of Continental Intraplate Seismicity: Insights from Geodynamic Modeling and Implications for Seismic Hazard Estimation. *Bulletin of the Seismological Society of America*, **99(1)**, 52-60.
- Liu, L. and M.D. Zoback (1997). Lithospheric strength and intraplate seismicity in the New Madrid seismic zone. *Tectonics*, **16**, 585-595.
- McBride, J.H. and K.D. Nelson (1988). Integration of COCORP deep reflection and magnetic anomaly analysis in the southeastern United States: Implications for origin of the Brunswick and East Coast magnetic anomalies. *Geological Society of America Bulletin*, **100**, 436-445.
- Miller, B.V., A.H. Fetter, and K.G. Stewart (2006). Plutonism in three orogenic pulses, Eastern Blue Ridge Province, southern Appalachians. *Geological Society of America Bulletin*, **118(1/2)**, 171-184.
- Mooney, W.D., J. Ritsema, and Y.K. Hwang (2012). Crustal seismicity and the earthquake catalog maximum moment magnitude (M_{cmax}) in stable continental regions (SCRs): Correlation with the seismic velocity of the lithosphere. *Earth and Planetary Science Letters*, **357-358**, 78-83.
- Olsen, P. E., R. W. Schlische, and P. J. W. Gore (1989). Tectonic, Depositional, and Paleogeological History of Early Mesozoic Rift Basins, *Eastern North America, Field Trip Guidebook T351*.

- Olsen, P. E., A.J. Froelich, D.L. Daniels, J.P. Smoot and P.J.W. Gore (1991). Rift basins of early Mesozoic age, in Horton, W., ed., *Geology of the Carolinas, University of Tennessee Press, Knoxville*, 142-170.
- Powell, C.A., G.A. Bollinger, M.C. Chapman, M.S. Sibol, A.C. Johnston, and R.L. Wheeler (1994). A Seismotectonic Model for the 300-Kilometer-Long Eastern Tennessee Seismic Zone. *Science*, **264(5159)**, 686-688.
- Raleigh, C.B., J.H. Healy, and J.D. Bredehoeft (1976). An Experiment in Earthquake Control at Rangely, Colorado. *Science*, **191**, 1230-1237.
- Rankin, D.W. (1976). Appalachian Salients and Recesses: Late Precambrian Continental Breakup and the Opening of the Iapetus Ocean. *Journal of Geophysical Research*, **81(32)**, 5605-5619.
- Rivers, T. (1997). Lithotectonic elements of the Grenville Province: review and tectonic implications. *Precambrian Research*, **86**, 117-154.
- Rutledge, J.T., W.S. Phillips, and M.J. Mayerhofer (2004). Faulting Induced by Forced Fluid Injection and Fluid Flow Forced by Faulting: An Interpretation of Hydraulic-Fracture Microseismicity, Carthage Cotton Valley Gas Field, Texas. *Bulletin of the Seismological Society of America*, **94**, 1817-1830.
- Sbar, M.L. and L.R. Sykes (1973). Contemporary Compressive Stress and Seismicity in Eastern North America: An Example of Intra-Plate Tectonics. *Geological Society of America Bulletin*, **84**, 1861-1882.
- Sigloch, K. (2011). Mantle provinces under North America from multifrequency P-wave tomography. *Geochemistry, Geophysics, Geosystems*, **12(2)**, Q02W08.

- Soller, D.R. (1988). Geology and tectonic history of the lower Cape Fear river valley, southeastern North Carolina. *United States Geological Survey Professional Paper*, **1466**.
- Swafford, L. and S. Stein (2007). Limitations of the short earthquake record for seismicity and seismic hazard studies. *Geological Society of America Special Paper*, **425**, 49-58.
- Sykes, L.R. (1978). Intraplate Seismicity, Reactivation of Preexisting Zones of Weakness, Alkaline Magmatism, and Other Tectonism Postdating Continental Fragmentation. *Reviews of Geophysics and Space Physics*, **16**, 621-688.
- Talwani, P. (1982). Internally consistent pattern of seismicity near Charleston, South Carolina. *Geology*, **10**, 654-658.
- Talwani, P. (1988). The intersection model for intraplate earthquakes. *Seismological Research Letters*, **59(4)**, 305-310.
- Tarr, A.C., P. Talwani, S. Rhea, D. Carver, and D. Amick (1981). Results of Recent South Carolina Seismological Studies. *Bulletin of Seismological Society of America*, **71**, 1883-1902.
- Thomas, W.A. (2006). Tectonic inheritance at a continental margin. *Geological Society of America Today*, **16(2)**, 4-11.
- van der Lee, S., K. Regenauer-Lieb, and D.A. Yuen (2008). The role of water in connecting past and future episodes of subduction. *Earth and Planetary Science Letters*, **273**, 15-27.
- Williams, H. and R.N. Hiscott (1987). Definition of the Iapetus rift-drift transition in western Newfoundland. *Geology*, **15**, 1044-1047.
- Wolin, E., S. Stein, F. Pazzaglia, A. Meltzer, A. Kafka, and C. Berti (2012). Mineral, Virginia, earthquake illustrates seismicity of a passive-aggressive margin. *Geophysical Research Letters*, **39**, L02305.

Zoback, M.L. (1992). Stress Field Constraints on Intraplate Seismicity in Eastern North America. *Journal of Geophysical Research*, **97(B8)**, 11761-11782.

7. Tables

Model	Distance (km)
1a	1.689
1b	2.093
1c	2.019
2	9.849
3	9.783
4	10.147
5	2.628
6	2.152
7	2.131

Table 1: The results of velocity model testing. Models 1-7 can be seen in Figure 5. Model 1a is Velocity Model 1 with all S-wave arrival picks and a free depth. Model 1b is Velocity Model 1 with Ranking 2 S-wave arrival picks removed and 1c is Velocity Model 1 with Ranking 2 S-wave arrival picks removed and depth fixed at 0 km. Distances are average distances to the events' respective source.

8. Figures

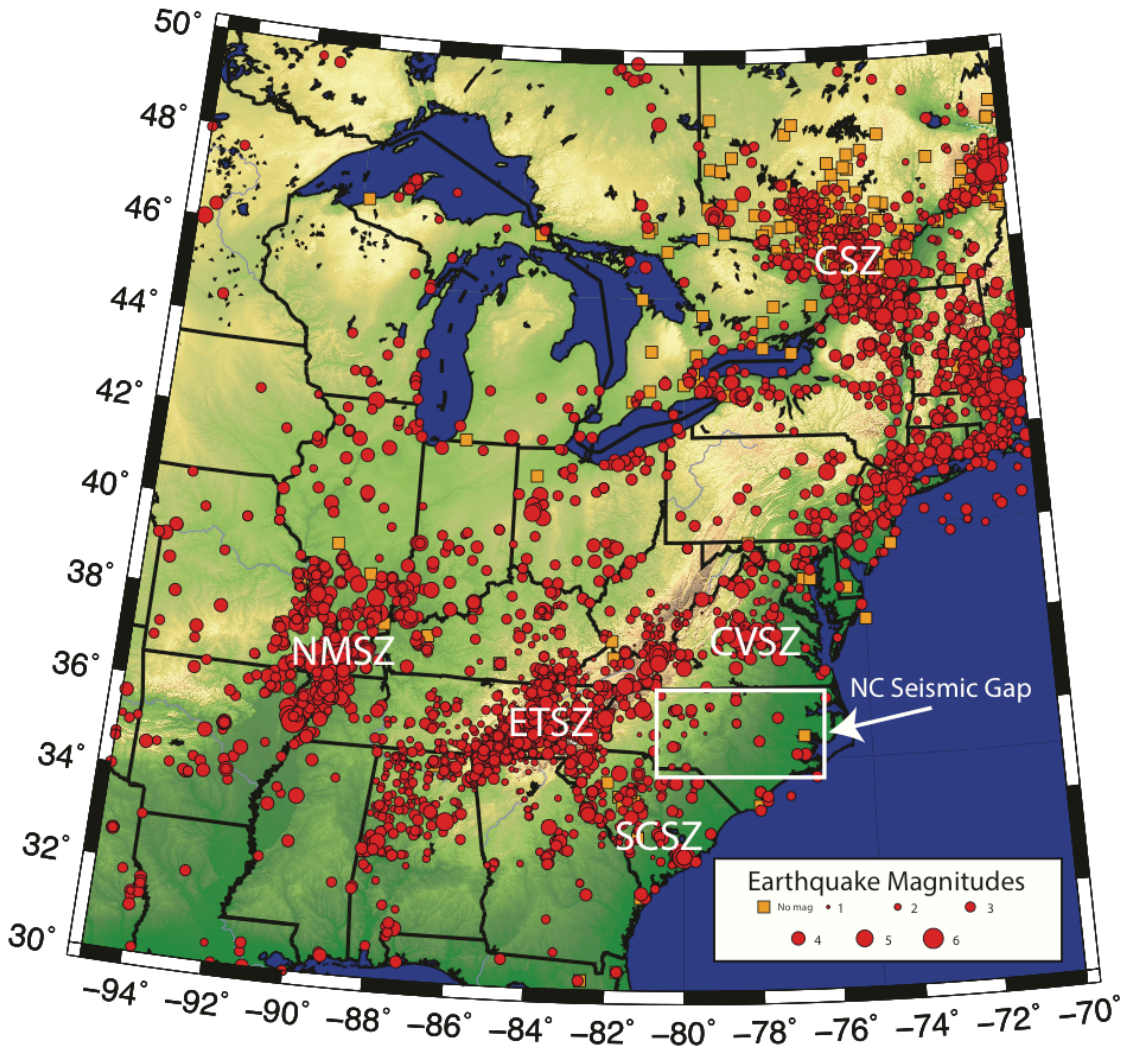


Figure 1: Map of seismicity in the eastern United States and Canada between 1568-2006 (www.geol.vt.edu/outreach/vtso/anonftp/catalog). The North Carolina seismic gap (NC Seismic Gap), South Carolina Seismic Zone (SCSZ), Eastern Tennessee Seismic Zone (ETSZ), Central Virginia Seismic Zone (CVSZ), New Madrid Seismic Zone (NMSZ) and Charlevoix Seismic Zone (CSZ) are each labeled.

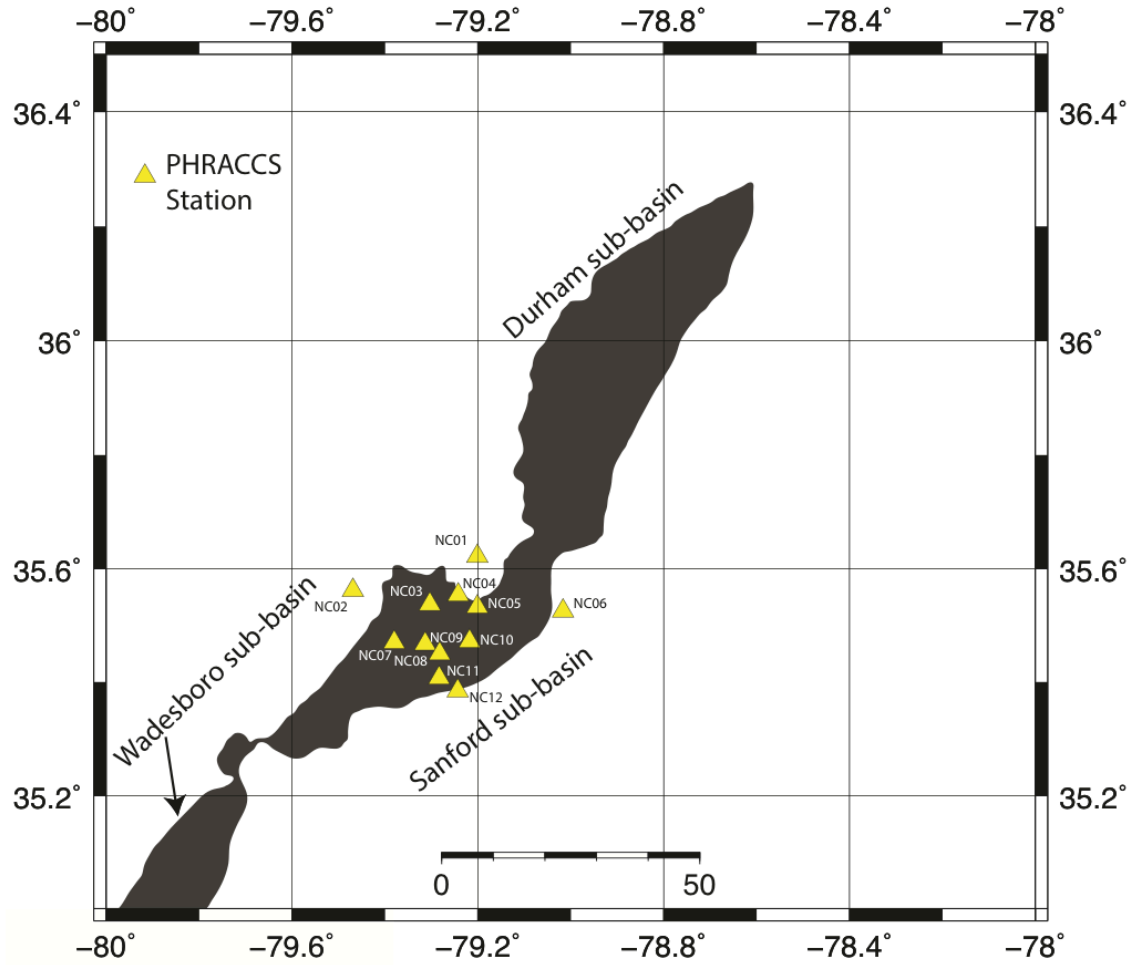


Figure 2: PHRACCS station map in relation to the Deep River Basin in North Carolina. Sub-basins are labeled.

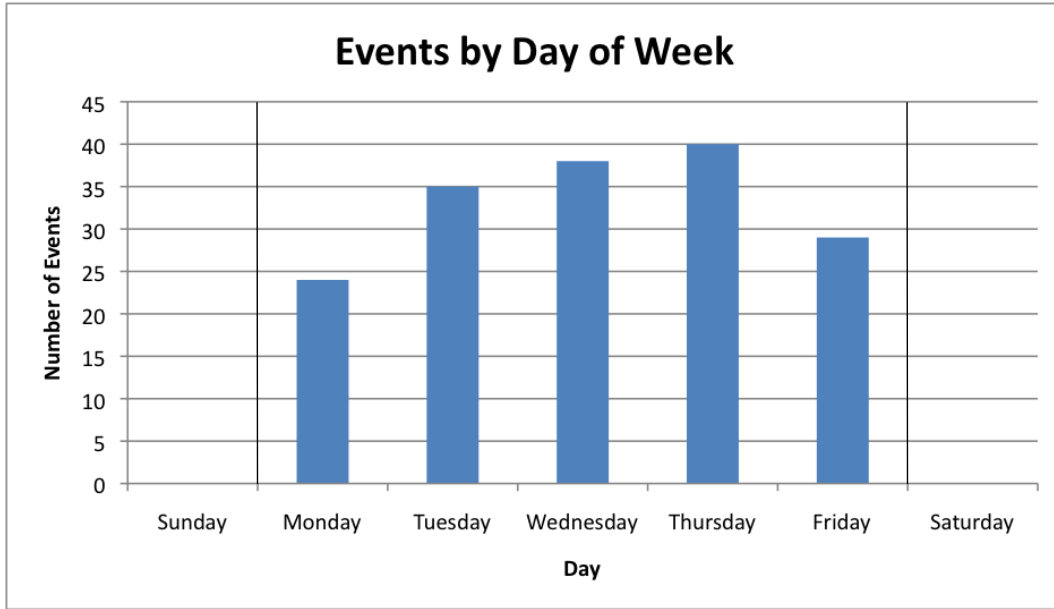


Figure 3: Histogram of events by day of the week. Black lines denote the common work week.

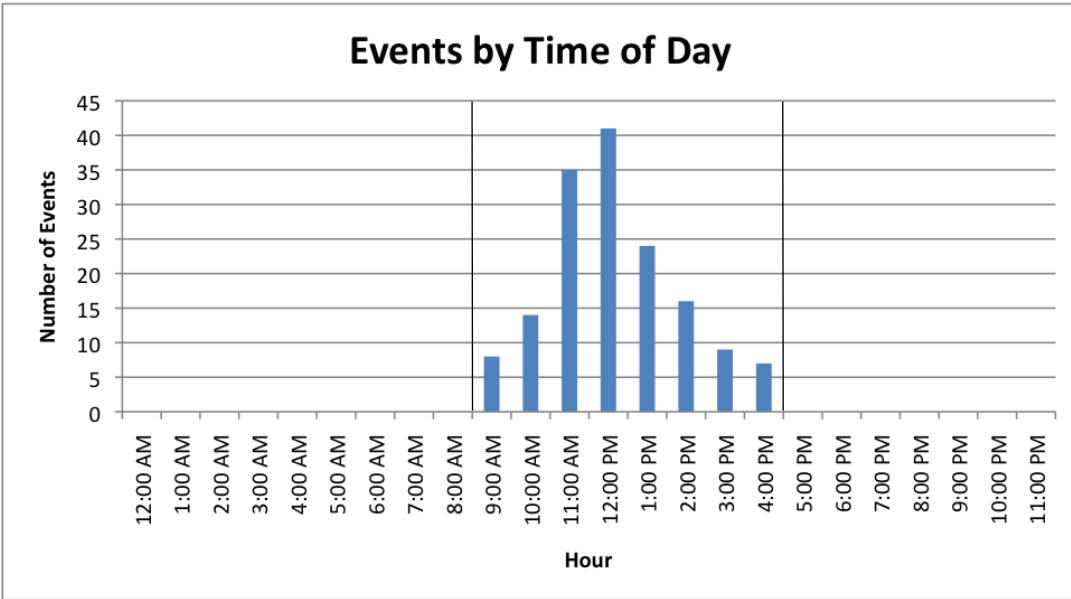


Figure 4: Histogram of events by time of day. Black lines denote the common work day.

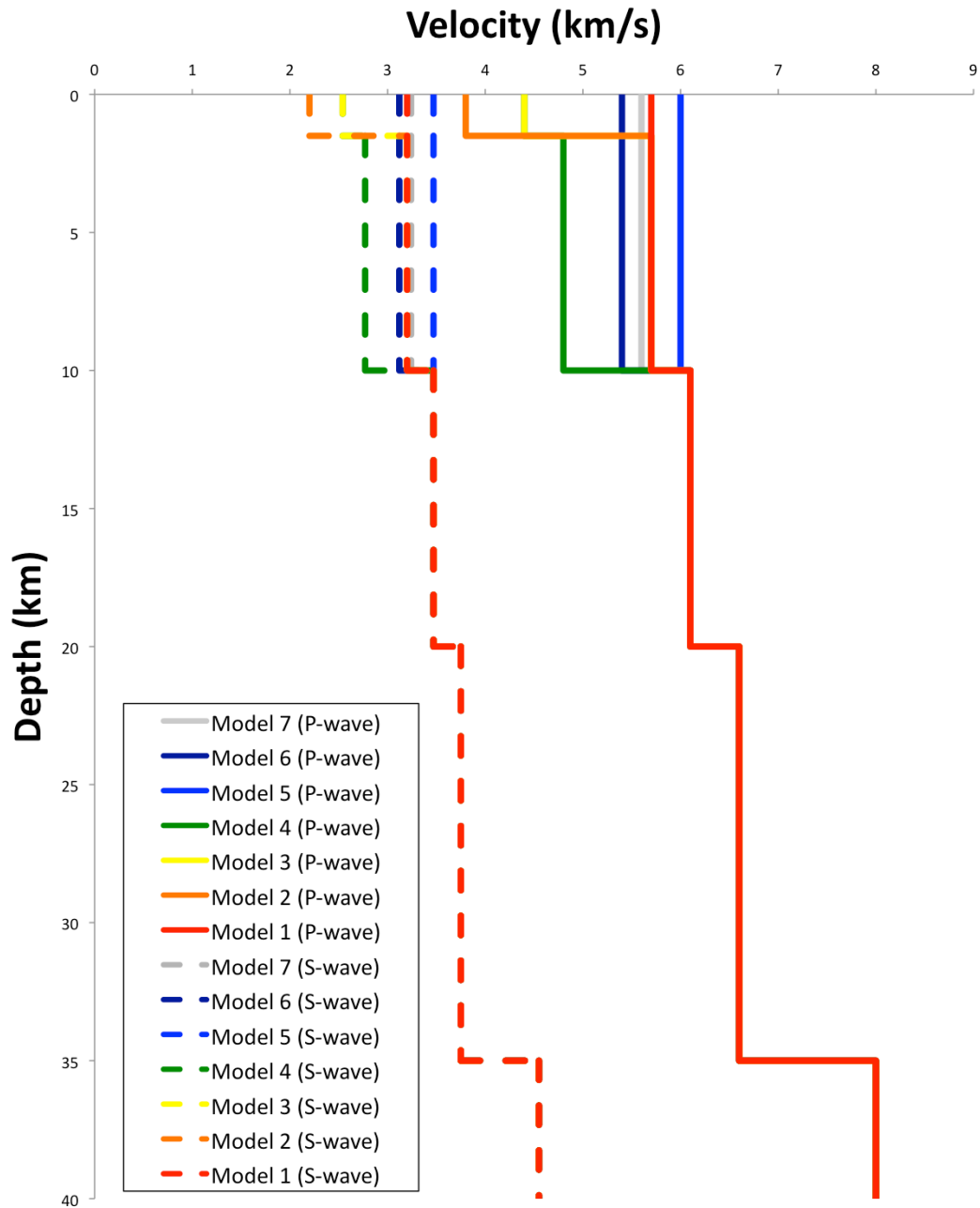


Figure 5: Velocity models tested. Solid lines are P-wave velocities for each model. Dashed lines are S-wave velocities for each model. The red lines represent the model used for locations in this study.

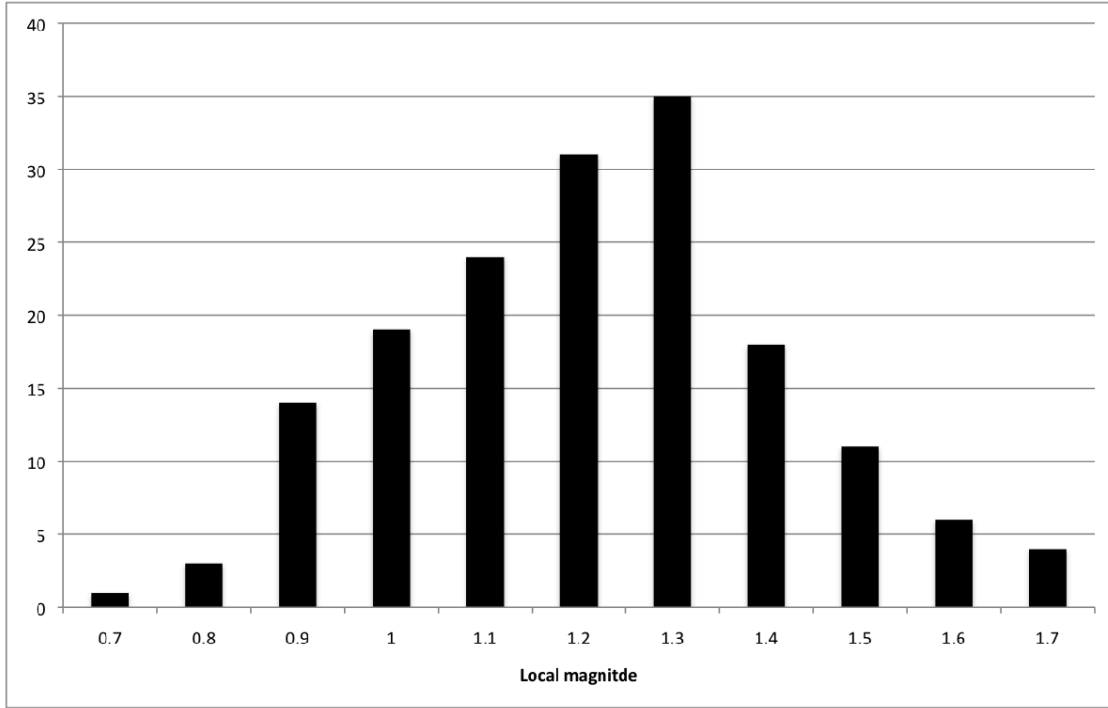


Figure 6: Histogram of calculated local magnitudes for all recorded events.

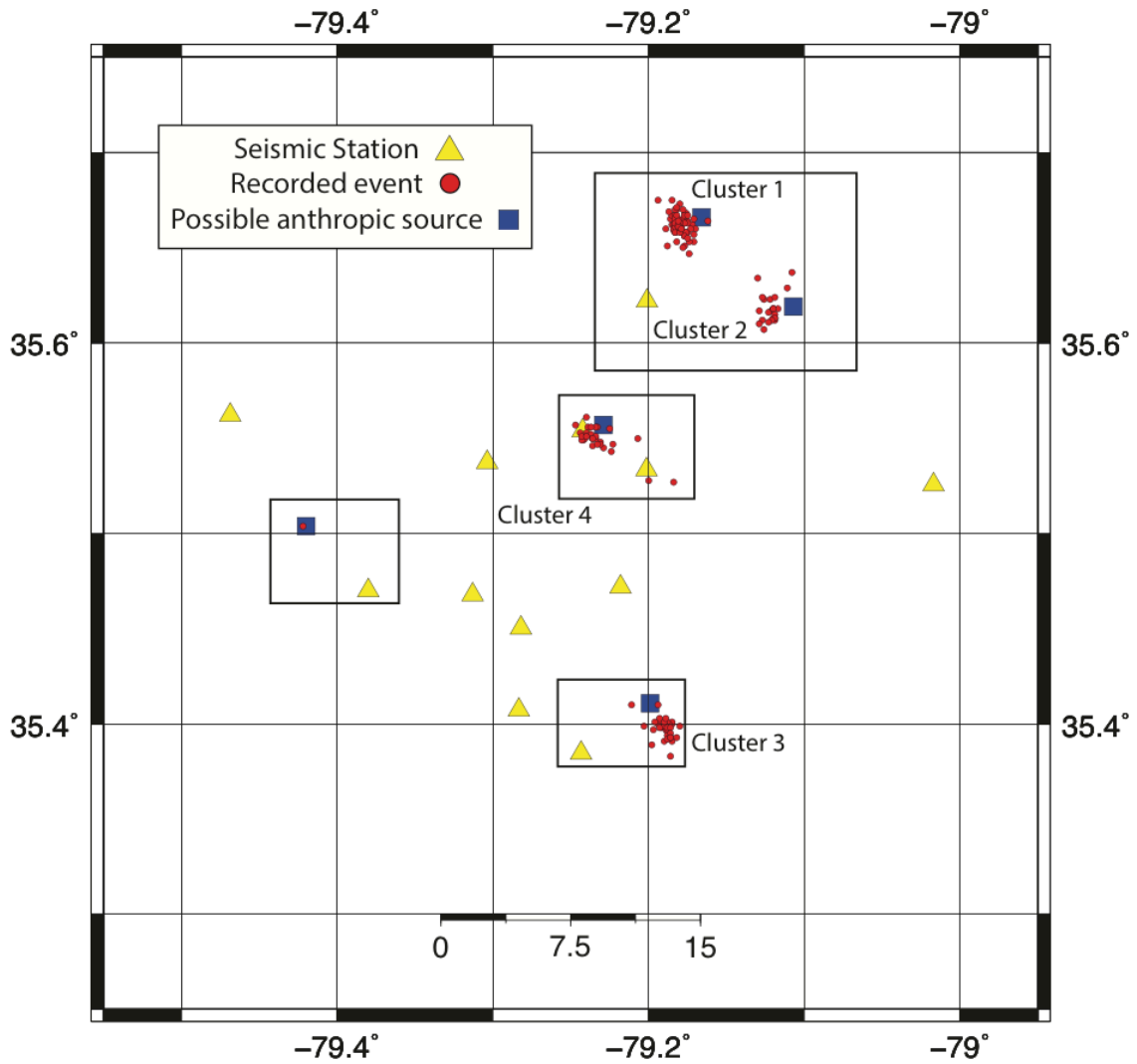


Figure 7: Map of recorded seismic events in relation to associated anthropogenic source and PHRACCS stations. The four clusters of events are labeled. Boxes show the locations of the satellite images in Figure 8.

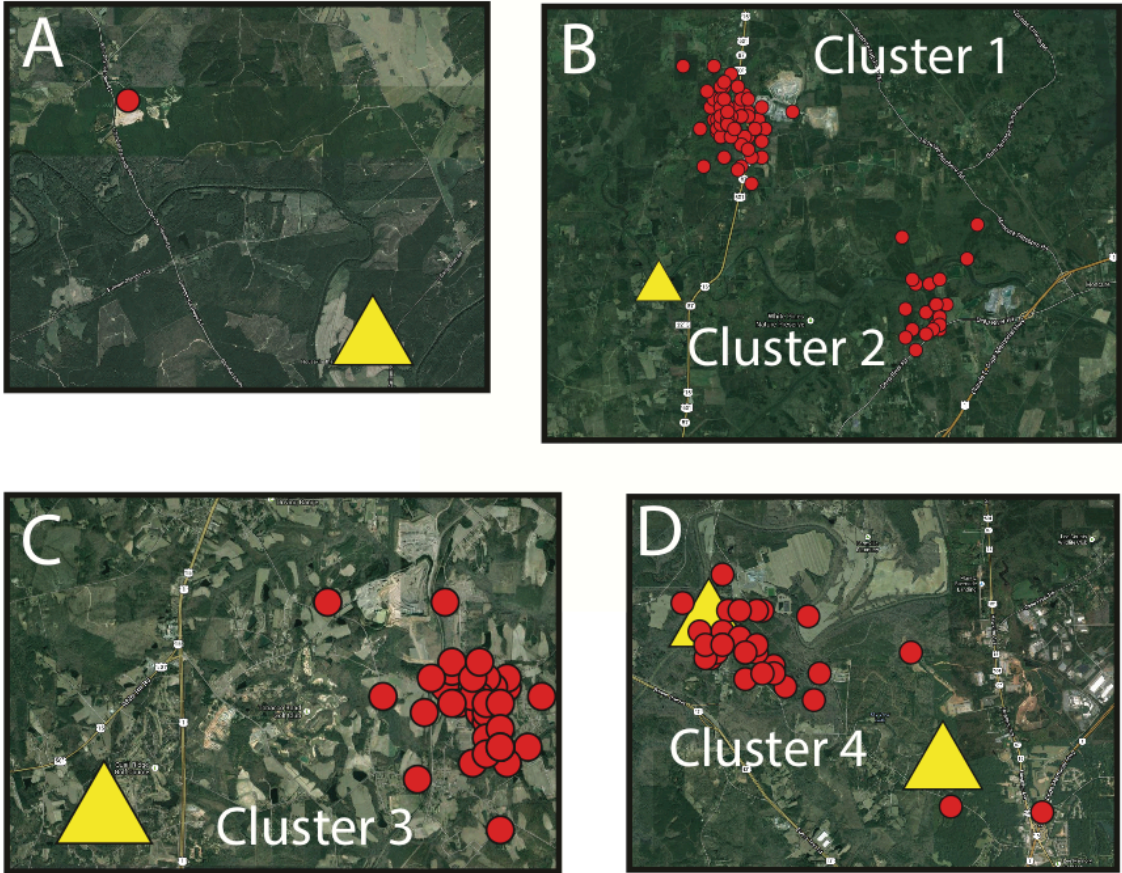


Figure 8: Satellite images from Google Maps showing each cluster of events. Each image shows anthropogenic sources for the seismicity.

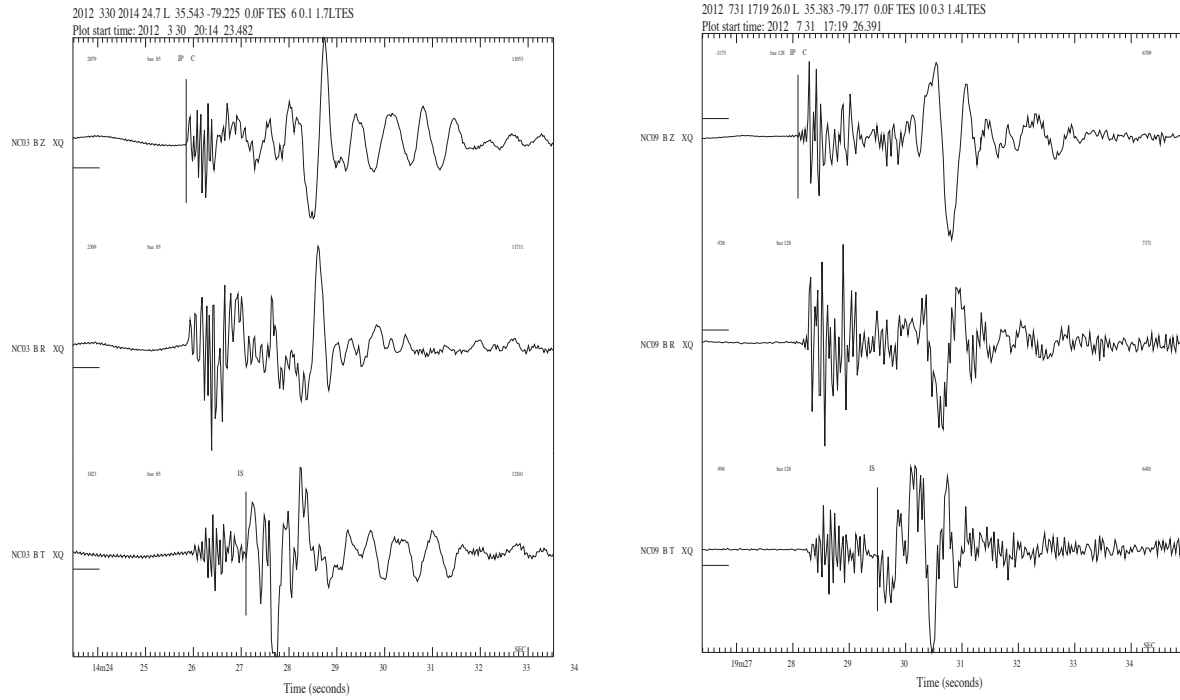


Figure 9: Sample seismograms of vertical, radial, and transverse components for a single station for two events. On the left are the seismograms recorded at station NC03 for an event in Cluster 4. On the right are the seismograms recorded at station NC09 for an event in Cluster 3. The event on the left does not have a confirmed source whereas the event on the right is confirmed as a quarry blast.

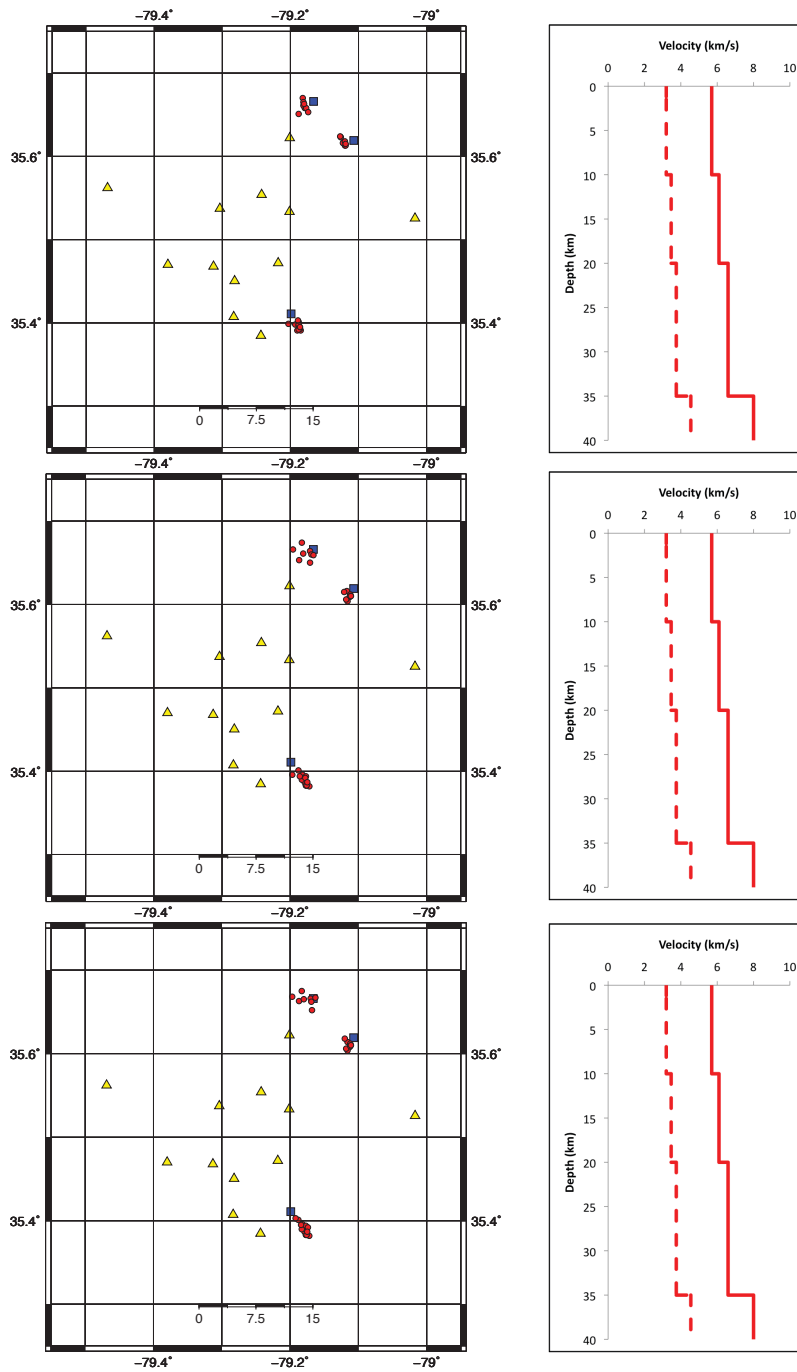


Figure 10: Maps showing event locations using each tested velocity model. On the left is the map and on the right is the corresponding velocity model, showing P-wave velocity with a solid line and S-wave velocity with a dashed line. Top is Velocity Model 1A, middle is Velocity Model 1B, and bottom is Velocity Model 1C.

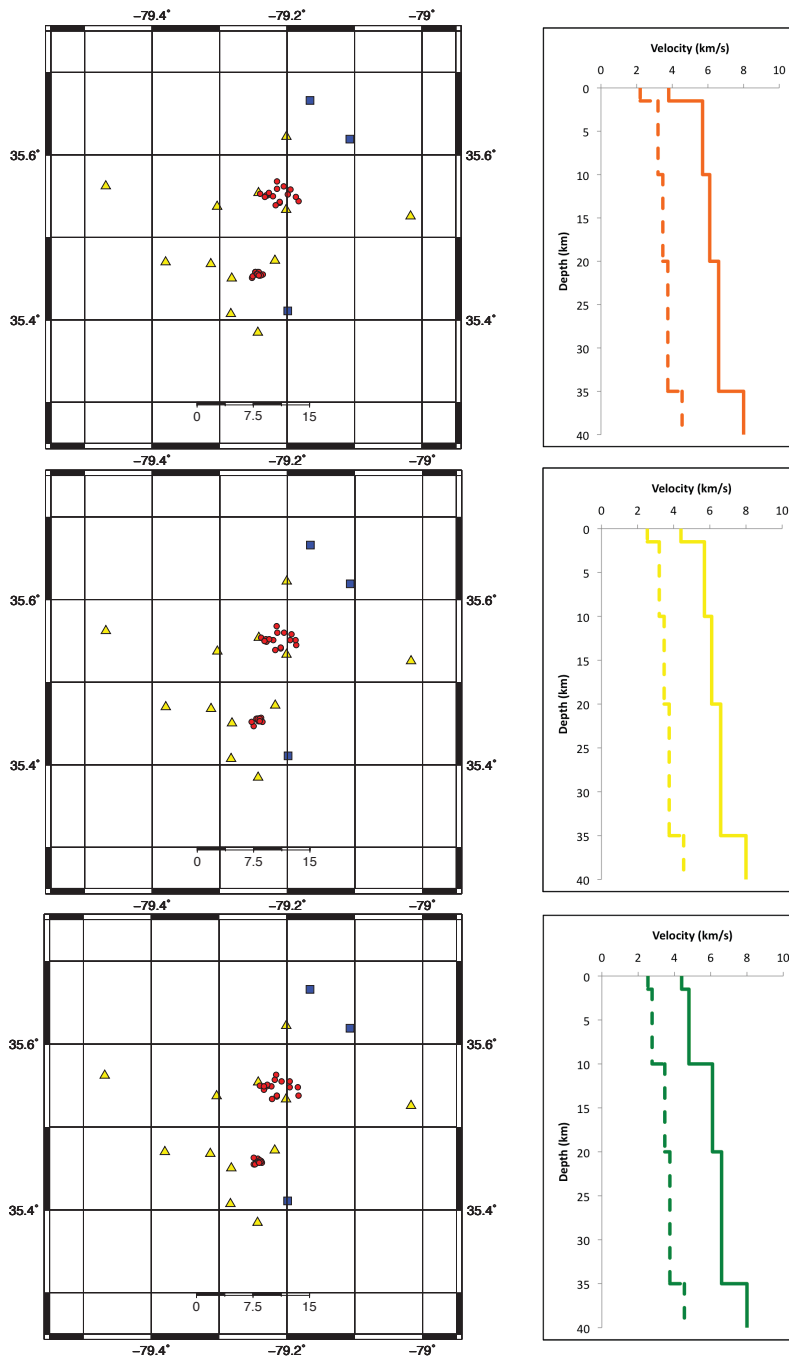


Figure 11: Maps showing event locations using each tested velocity model. On the left is the map and on the right is the corresponding velocity model, showing P-wave velocity with a solid line and S-wave velocity with a dashed line. Top is Velocity Model 2, middle is Velocity Model 3, and bottom is Velocity Model 4.

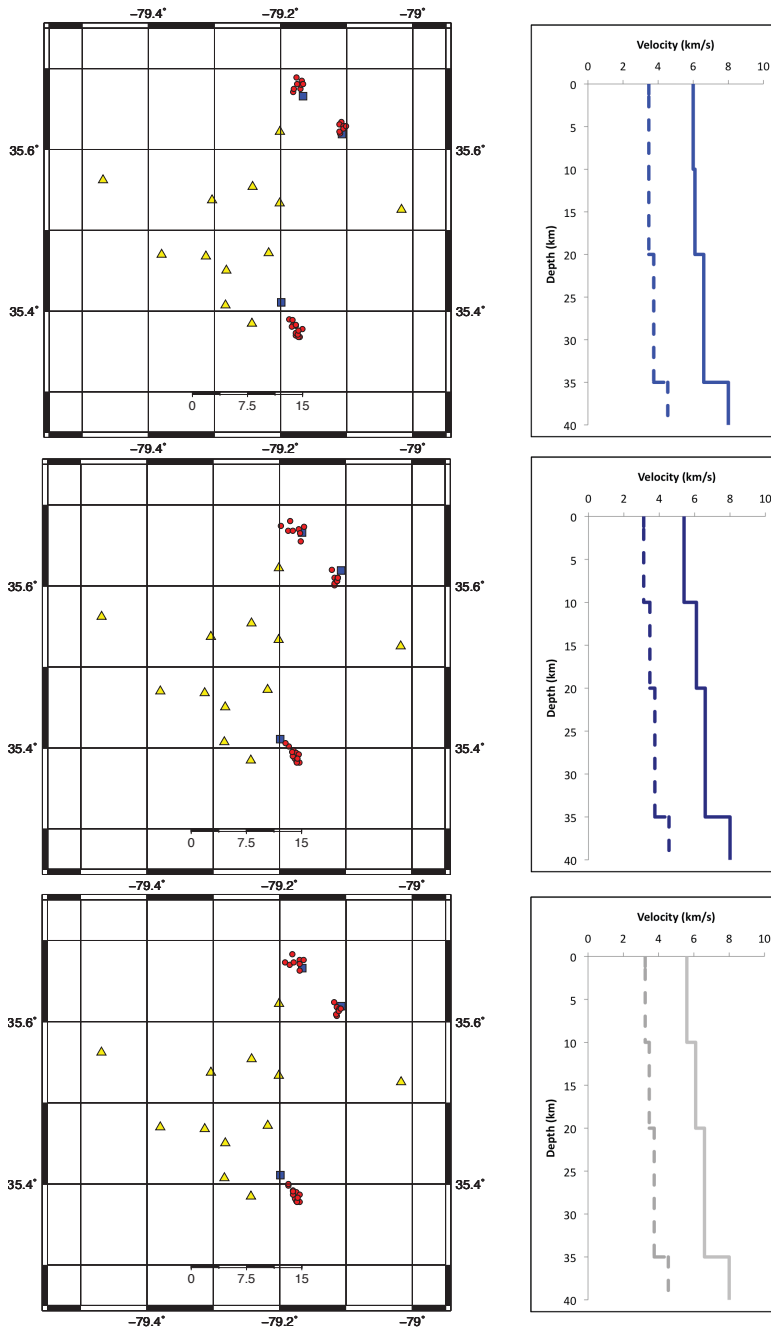


Figure 12: Maps showing event locations using each tested velocity model. On the left is the map and on the right is the corresponding velocity model, showing P-wave velocity with a solid line and S-wave velocity with a dashed line. Top is Velocity Model 5, middle is Velocity Model 6, and bottom is Velocity Model 7.

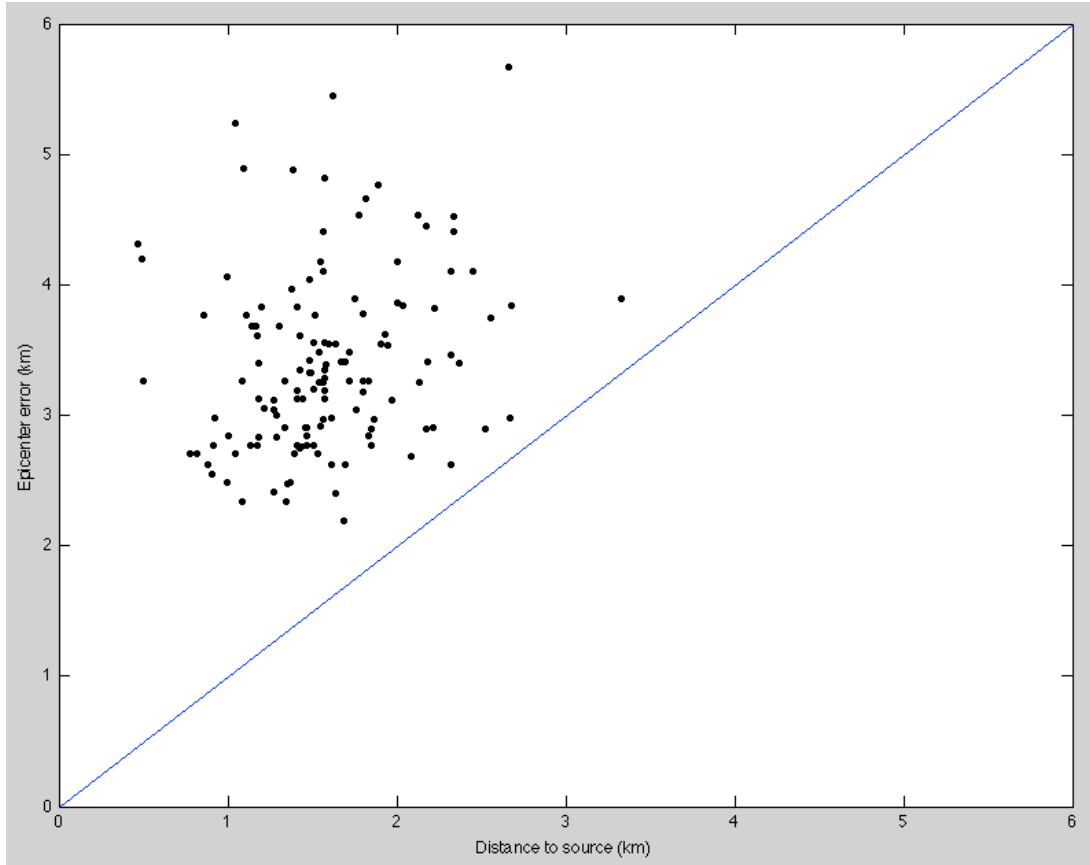


Figure 13: Plot of calculated epicenter error (km) versus distance to event source (km). The blue line is a simple line of $y = x$. Events plotted above the line were located accurately within error. Only events with a known source location were included.